Molecular Structure and Shear Rheology of Long Chain Branched Polypropylene Formed by Light Cross-Linking of a Linear Precursor with 1,3-Benzenedisulfonyl Azide

Jens Kjær Jørgensen,[1] Keith Redford,[2] Espen Ommundsen,[3] Aage Stori[2]

[1]*Department of Engineering Design and Materials, Norwegian University of Science and Technology, 7491 Trondheim, Norway*
[2]*SINTEF Materials and Chemistry, 0314 Oslo, Norway*
[3]*Borealis AS, 3960 Stathelle, Norway*

Received 29 September 2006; accepted 2 April 2007
DOI 10.1002/app.26674
Published online 3 July 2007 in Wiley InterScience (www.interscience.wiley.com).

ABSTRACT: Linear isotactic metallocene based polypropylene (M_w = 125,000 g/mol, M_n = 61,000 g/mol) was lightly crosslinked by small amounts of 1,3-benzenedisulfonyl azide to form long chain branches (LCB). Crosslinking was carried out by reactive extrusion at 200°C in a small scale extruder. At the processing temperature, the two azide groups decompose to nitrenes that work as crosslinkers for PP. The crosslinking reaction occurs primarily by insertion of singlet nitrenes into C—H bonds. 1,3-benzenedisulfonyl azide concentrations of, respectively, 518, 806, 1029, and 2038 ppm were used. SEC revealed formation of a high molecular weight LCB fraction. No degradation was observed by SEC. The introduction of LCB gave rise to rheological behavior typical of LCB as increased zero shear viscosity, accompanied by increased shear thinning, increased flow activation energy and a phase angle plateau. However, the rheological impact and crosslinking efficiency observed were limited compared to earlier studies on PE. Possible reasons for this are discussed. © 2007 Wiley Periodicals, Inc. J Appl Polym Sci 106: 950–960, 2007

Key words: branched; gel permeation chromatography (GPC); polyolefins; reactive extrusion; rheology

INTRODUCTION

Polypropylene (PP) is one of the world's most important thermoplastics and its market share is growing. This is as a result of its desirable properties such as low cost, high melting point, low density, high tensile strength and stiffness, and excellent chemical resistance. However, since almost all commercial PP is linear and therefore has low melt strength, its use is limited in processes with large extensional deformations such as foaming, extrusion coating, film blowing, and blow molding. In recent years, metallocene catalyzed PP (mPP) with improved mechanical properties has been developed. A problem with mPPs is that their narrow molecular weight distribution leads to low degree of shear thinning and thereby low process-ability. For polyethylene both of these problems can and are widely being solved by the introduction of long-chain branching (LCB) in the molecular structure.[1] Efforts have also been made to introduce LCB in PP and some commercial grades are available. Nevertheless, since radicals lead to degradation of PP, the LCB forming processes are more complicated for PP than for PE which is crosslinked by radicals. At present the methods reported to make LCB-PP are: crosslinking by reactive extrusion with disulfonylazides[2,3] or with certain peroxydicarbonates,[4] electron beam radiation of blends of PP and some polyfunctional monomer,[5,6] copolymerization of propylene with dienes[7,8] or by incorporation of vinyl-terminated chains during synthesis with metallocene catalysts.[9] The use of disulfonyl azides to crosslink PP has mainly been addressed in patents,[2] and only sparsely described in scientific journals.[3,10] In this paper, we consider characterization of the long-chain branching structure formed in linear isotactic PP crosslinked with 1,3-benzenedisulfonyl azide (1,3-BDSA) (Fig. 1), and its impact on rheological properties. The paper is our third paper concerning crosslinking of polyolefins with 1,3-BDSA. Previously we have studied reaction mechanisms and kinetics of 1,3-BDSA undergoing thermal decomposition in a polyolefin[10] and molecular structure and rheological properties of PE lightly crosslinked with 1,3-BDSA to form LCB.[11]

Correspondence to: J. K. Jørgensen (jens.k.jorgensen@sintef.no).

Contract grant sponsors: Borealis AS, The Research Council of Norway.

Journal of Applied Polymer Science, Vol. 106, 950–960 (2007)

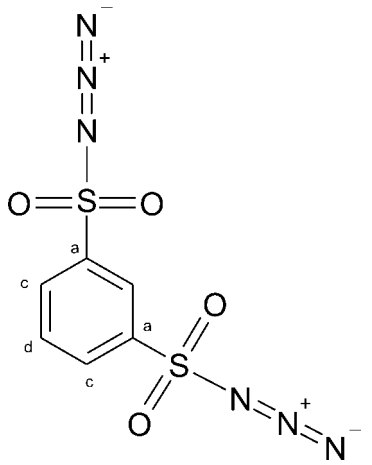

Figure 1 Chemical structure of 1,3-benzenedisulfonyl azide.

Reactions of 1,3-BDSA with hydrocarbons

The ability of disulfonyl azides to crosslink hydrocarbon polymers has been recognized since the sixties.[12] In our earlier paper, we investigated and discussed the reaction involved when 1,3-BDSA decompose in a polyolefin.[10] Our findings were in agreement with earlier reports.[13,14] At elevated temperature sulfonyl azides decompose to form a sulfonyl nitrene as shown in Scheme 1. The nitrene can exist in both singlet and the triplet state. The singlet nitrene can attach directly to a hydrocarbon chain by insertion at the C—H bond, resulting in a secondary sulfonyl amide (Scheme 2). If both nitrene groups on a disulfonyl nitrene perform this action, a crosslink is formed. Triplet nitrenes can also be involved in crosslinking. However, this takes place through a number of reactions that can also lead to degradation. First step is abstraction of a hydrogen molecule from the hydrocarbon, resulting in formation of a macroradical [Scheme 3(a)]. A possible reaction following this is combination of the products of Scheme 3(a) [Scheme 3(b)], resulting in the same type of bond as formed by the singlet nitrene. Another possibility is abstraction of a second hydrogen from the same or another hydrocarbon to form a second macroradical and stable primary sulfonyl amide [Scheme 3(c)]. If the macroradicals combine, a crosslink is formed just as desired. Nevertheless, since PP macroradicals are very likely to decompose at the radical carbon, Schemes 3(a) and (c) are unwanted reactions.

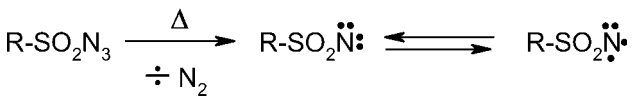

Scheme 1 Formation of singlet and triplet nitrenes from azide.

Scheme 2 Reaction of singlet nitrene with hydrocarbon. Formation of secondary sulfonyl amide.

However, our earlier studies[10] suggest that crosslink-forming reactions are dominant. With insufficient blending nitrene–nitrene reactions can occur thereby reducing the number of nitrenes available for crosslinking.[10,15] Also, the presence of oxygen should be avoided, since it reacts very efficiently with nitrenes to form nitroso compounds.[10,15] The simplest branching structure rising from these reactions will be four armed stars with 1,3-BDSA as the center point and arm lengths dependent on the length of the two linear precursors and the position of the crosslink along these chains. For high concentration of 1,3-BDSA or if local clusters of 1,3-BDSA exist, more complex structures will also appear. Intrachain crosslinking will evidently take place to some extent. This can lead to complex structures such as loops that in some cases resemble long chain branches.

Rheology and LCB

LCB has a pronounced effect on the melt flow properties of polymer melts that can be beneficial in polymer processing. The properties of LCB containing polyolefins have been extensively studied in the past years and the results have been reviewed by a number of authors.[1,16] These studies mainly concern polyethylene and copolymers thereof, while studies on LCB-PP are more limited.[5–9,17–22] Anyway the effects are qualitatively the same for PE and PP. The origin of the high impact of LCB on melt flow lies in their ability to form entanglements that restrict the linear

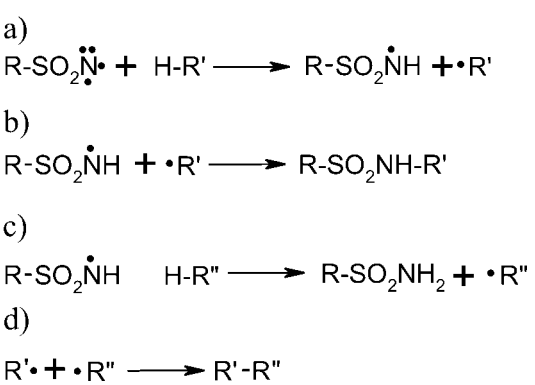

Scheme 3 Reaction of triplet nitrene with hydrocarbon. (a) Formation of macroradical by H-abstraction. (b) Formation of secondary sulfonyl amide by recombination. (c) Formation of primary sulfonyl amide by abstraction of a second hydrogen. (d) Combination of macroradicals formed by reaction (b) and (c), mechanical cleavage or in other ways.

reptition motion of the chain along its tube.[23] Instead the motion of the branched chain takes place by retraction of the arms, a process giving rise to much longer relaxation time than for linear chains. This also relates to the rheological definition of LCB as branches of the critical entanglement molecular weight (M_c) or higher molecular weight. The most common effect of LCB is increased zero shear viscosity η_o accompanied by increased shear thinning when comparing linear and LCB species of the same molecular weight.[5,7,21,24,25] The strong entanglements formed in LCB containing polymers make their melts more elastic and stronger than for linear polymers. This gives rise to increased shear recoverable compliance J_e^o,[26–28] and strain hardening in extensional flow.[17,21] Another consequence of LCB is increased flow activation energy E_a[27,29,30] and thermorheological complexity.[30–32]

EXPERIMENTAL

Materials

Linear isotactic metallocene polypropylene from now on referred to as PP0 was supplied by Borealis AS as unstabilized reactor powder. To avoid degradation, the powder was kept in darkness and at −20°C. Before processing, PP0 was stabilized with 800 ppm Irganox 1010® (hindered phenol) dissolved in acetone, 1200 ppm Irgafos 168® (phosphite) dissolved in dichloroethane, and 900 ppm calcium stearate dispersed in acetone. The stabilizers were supplied by Ciba Specialty Chemicals.

Crosslinking procedure

PP0 was modified with concentrations of 518, 806, 1029, and 2038 ppm 1,3-BDSA. From elementary stoichiometric calculations one finds that 1 ppm of 1,3-BDSA corresponds to 0.000,049 1,3-BDSA/10,000 carbon. The number of 1,3-BDSA/10,000 backbone carbon for the respective samples are listed in Table I. The crosslinking was carried out by reactive extrusion at 200°C. The steps of the crosslinking procedure were the following: 1,3-disulfonyl-azidobenzene was dissolved in acetone. The solution was added to PP0 powder and blended thoroughly into the powder. After evaporation of the acetone, the blend was extruded in a DSM2000 mini extruder at 70 rpm. This is a 15 cm^3 twin screw extruder with feedback that is suited for blending of small batches. The extrusion lasted for 6 min which is enough to reach full conversion at 200°C.[10] Twenty-five mm discs for rheology analysis were prepared directly after the extrusion by injection molding in a DSM Minimat injection molding machine.

Size exclusion chromatography

Molecular weight distributions (MWD) and LCB-distributions were determined by size exclusion chromatography (SEC). This was performed on a Polymer Laboratories GPC 210 equipped with a PL differential refractometer (DRI), a two angle (15° and 90°) Precision Detector PD2040 light scattering detector (LSD) and a Viscotec 150R differential bridge viscometer detector (VD). All detectors were situated in the oven compartment. The LSD was placed immediately after the columns followed by the DRI and the VD in parallel with a ~40:60 flow split. The columns used were a set of four Plgel 20 μm MIXED-A LS 300 × 7.5 mm and a Plgel 20 μm Guard 300 × 7.5 mm. 1,2,4-trichlorobenzene (TCB) stabilized with 0.02 wt % 2,6-di-*tert*-butyl-*p*-cresol (BHT) was used as solvent. The analyses were performed at 145°C with a flow rate of 1.00 mL/min. Columns and detectors were calibrated using 14 narrow polystyrene (PS) standards supplied by Polymer Laboratories with molecular weights ranging from 600 to 2×10^6. A 200-μm injection loop was used for all measurements.

Samples for GPC were prepared by dissolving an accurate amount of ~ 20 mg of sample in 20 mL of TCB stabilized with 0.02 wt % BHT. Dissolution of the samples was achieved within 1.5 h at 160°C.

PP0 contained catalyst residues. To avoid column frit blockage from these particles (10 μm column frit), all samples were filtered at 145°C in a hot filtration device consisting of a syringe and filter in a heated block. The filters used were 5 μm MITEX PTFE discs from Millipore contained in a Swinney Stainless Filter Holder.

TABLE I
Results of SEC Analyses

Sample	[1,3-BDSA] (ppm)	M_n (10^3 g/mol)	M_w (10^3 g/mol)	PD	g_w	g'_w	β_w (branch points/ molecule)	λ_w (branch points/10^4 carbon)	1,3BDSA/10^4 carbon	ε
PP0	0	61	125	2.1				0	0	
PP518	518	59	131	2.2	0.995	0.993	0.02	0.01	0.25	1.3
PP806	806	57	136	2.4	0.990	0.985	0.04	0.03	0.39	1.36
PP1029	1029	58	144	2.5	0.989	0.984	0.05	0.02	0.50	1.40
PP2038	2038	74	244	3.3	0.957	0.939	0.24	0.07	0.99	1.45

GPC data were analyzed with PL Cirrus software and in house software with equivalent results. To improve the quality of the data, raw data of several runs for each sample were averaged, before the data analyses. Molecular weights M were determined from the standard equation for static light scattering[33]

$$\frac{Kc}{\Delta R(\theta, c)} = \frac{1}{MP(\theta)} + 2A_2c \quad (1)$$

$\Delta R(\theta,c)$ is the excess Rayleigh ratio at angle θ, c is the polymer concentration, and A_2 the second virial coefficients of the polymer solution. For PP in TCB, we used $A_2 = 1 \times 10^{-3}$ mol cm^3 g^{-2}. $P(\theta)$ is the form factor. For a Gaussian coil with a mean square radius of gyration $\langle R_g{}^2\rangle^{1/2}$ it is given by

$$P(\theta) = \frac{2}{\left(q^2\langle R_g^2\rangle\right)^2}\,[q^2\langle R_g^2\rangle - 1 + \exp\left(-q^2\langle R_g^2\rangle\right)], \quad (2)$$

where

$$q = \frac{4\pi n}{\lambda}\sin\left(\frac{\theta}{2}\right). \quad (3)$$

Here q is the modulus of the scattering vector, n the refractive index of the solution, and λ wavelength of the laser in vacuum. $P(\theta)$ and $\langle R_g{}^2\rangle^{1/2}$ were determined from the dissymmetry method for dual angle light scattering.[34] At low molecular weights, the uncertainty in $\langle R_g^2\rangle^{1/2}$ determined from light scattering increases strongly. Due to this $\langle R_g^2\rangle^{1/2}$ in the low molecular region was calculated from the Flory–Fox equation

$$[\eta] = 6^{3/2}\phi\langle R_g^2\rangle^{3/2}M^{-1}. \quad (4)$$

With a Flory–Fox constant $\phi = 2.3 \times 10^{21}$ dL mol^1 cm^3, $<R_g^2>^{1/2}$ in the high molecular weight region found from eq. (4) fitted nicely with those found directly from light scattering.

Rheometry

Rheological properties were measured with a *Paar Physica* MCR 300 rheometer using parallel plate geometry. Plate diameter was 25 mm and plate thickness 1 mm. Strain controlled dynamic measurements and creep measurements were performed. Appropriate strain amplitudes within linear viscoelastic responses were determined from strain sweeps at 0.06–600 rad/s.

RESULTS AND DISCUSSION

The samples discussed are named after the convention PP[concentration of 1,3-BDSA in ppm].

Gel measurement

The most crosslinked sample was examined for content of gel due to ASTM 2765. The basis of this method is to pack the sample in a copper net and extract the polymer in boiling *para*-xylene. Gel particles larger than the net mesh will be left in the net. No gel was measurable with this method using a 100-μm mesh size.

Molecular weight distributions

Average molecular weights obtained from SEC analyses are listed in Table I. Molecular weight distributions of the linear precursor PP0 and the modified samples are shown in Figure 2. As expected the crosslinking results in the formation of a high molecular weight fraction that increases with the amount of crosslinking.

Random crosslinking

If the sulfonyl azide is well dispersed and randomly distributed into the polymer, we expect the crosslinking process to be random. How the molecular structure develops during random crosslinking of a linear chains with a bifunctional crosslinker influence has been studied theoretically. Macosko and Miller[35] and Tobita[36] found by different methods

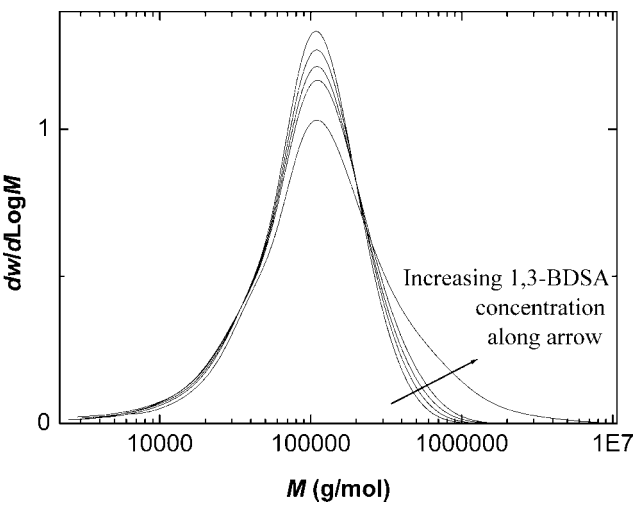

Figure 2 Molecular weight distributions of crosslinked PP and the linear precursor. 1,3-BDSA concentration increases along the arrow in the order 0, 518, 806, 1029, 2038 ppm.

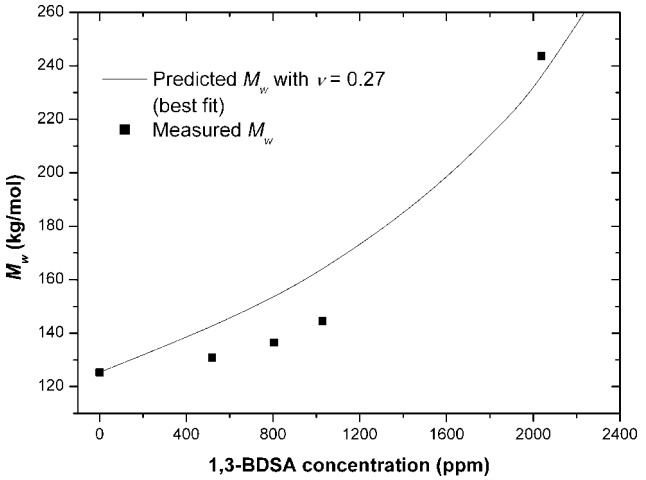

Figure 3 Weight average molecular weights M_w measured with SEC-LS compared with values predicted from random crosslinking theory with 27% crosslinking efficiency of 1,3-BDSA.

that the weight average degree of polymerization P_w grows as

$$P_w = \frac{P_{\mathrm{wp}}(1+\rho)}{1-(P_{\mathrm{wp}}-1)\rho}. \tag{5}$$

P_{wp} is the weight average degree of polymerization of the linear precursor and ρ is the crosslinking density defined as

$$\rho = \frac{\text{number of crosslinked monomers}}{\text{total number of monomers}} \tag{6}$$

One should note that one crosslink contains two crosslinked monomers. In the derivation of eq. (5), it is assumed that all monomers have the same probability to be crosslinked, but that no intrachain crosslinking occurs. In the ideal case the number of crosslinked monomers should be the double of the number of crosslinkers. In reality the efficiency of the crosslinker ν can be described by some value between zero and one related to ρ as

$$\rho = \nu\,\frac{2\times\text{number of crosslinkers}}{\text{total number of monomers}} \tag{7}$$

Hence, from the above equations and measured values of $P_w/P_{\mathrm{wp}} = M_w/M_{\mathrm{wp}}$ ν can be estimated (M_w and M_{wp} are weight molecular weight averages of the crosslinked polymer and the linear precursor, respectively). Figure 3 shows how the M_w of our crosslinked samples develop with increasing crosslinking. The measured values fit fairly well with those predicted from random crosslinking with a crosslinking efficiency $\nu = 0.26$ (best fit). However, the measured M_w as a function of crosslinker concentration clearly exhibit a larger second derivative than the theoretically predicted M_w. In other words the crosslinking efficiency deduced from eqs. (5)–(7) increases with the concentration of 1,3-BDSA. We consider whether this discrepancy could be a result of intrachain crosslinking which in eq. (5) is neglected. In a polymer melt under no deformation the polymer chains exist in an unperturbed random coil state with overlap between different chains. In that case the probability of intrachain crosslinking will not change throughout a crosslinking process. In reactive extrusion, the blend is deformed and the polymer chains stretched due to entanglements. Large and especially long chain branched chains have strong entanglements and will be stretched more and have longer relaxation times than short linear chains. As the crosslinking process proceeds entanglements increase in number and more chains will be stretched and thereby be less exposed to intrachain crosslinking. Thus, due to these arguments the crosslinking efficiency can increase with crosslinker concentration due to decreased intrachain crosslinking. The question is of course how strong this effect is.

According to the model of random crosslinking with $\nu = 0.26$ (best fit) an infinite network ($M_w = \infty$) is formed at a critical concentration of 4370 ppm crosslinker. However, the measured M_w's overshoot the model with increased crosslinking. Therefore, this critical concentration is probably even lower and close to our maximum concentration of 2038 ppm.

Long chain branching

The amount of LCB can be determined from $\langle R_g^2\rangle^{1/2}$ and intrinsic viscosity [η] measured by SEC equipped with light scattering or viscosity detector, respectively. Branched polymer chains in solution are more dense and have lower R_g and [η] than linear chains of the same molecular weight. This is expressed through the contraction factors

$$g = \frac{\langle R_g^2\rangle_{\mathrm{br}}}{\langle R_g^2\rangle_{\mathrm{lin}}} \tag{8}$$

$$g' = \frac{[\eta]_{\mathrm{br}}}{[\eta]_{\mathrm{lin}}}. \tag{9}$$

Here the suffixes *br* and *lin* represent branched and linear. g and g' are related as

$$g' = g^{\varepsilon}, \tag{10}$$

where ε takes values between 0.5 and 1.5 dependent on branching type and density. g is directly related to the number of LCB per polymer chain, given that

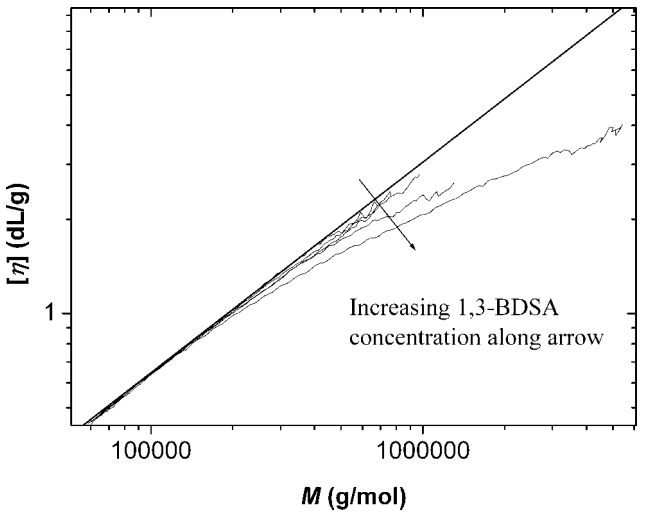

Figure 4 Intrinsic viscosity [η] versus molecular weight of linear PP crosslinked with 1,3-BDSA. Each curve represents values for samples of the linear precursor modified with a certain concentration of 1,3-BDSA. 1,3-BDSA concentration increases along the arrow in the order 0, 518, 806, 1029, 2038 ppm. The straight line represents a linear fit to [η] of the linear precursor.

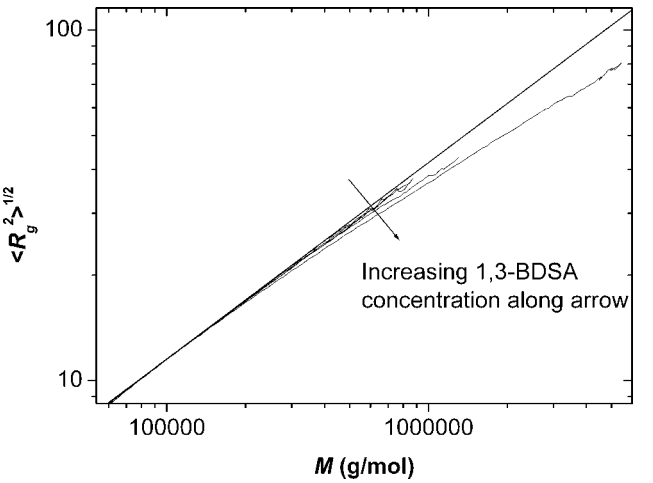

Figure 5 Root mean-square radius of gyration $\langle R_g^2 \rangle^{1/2}$ versus molecular weight of linear PP crosslinked with 1,3-BDSA. Each curve represents values for samples of the linear precursor modified with a certain concentration of 1,3-BDSA. 1,3-BDSA concentration increases along the arrow in the order 0, 518, 806, 1029, 2038 ppm. The straight line represents a linear fit to $\langle R_g^2 \rangle^{1/2}$ of the linear precursor.

they have the same type of branching structure. For four-functional branching as we expect from modification with 1,3-BDSA, g is related to the weight–average number of branch points β at a fixed molar weight as[37]

$$g_4 = \left[\left(1 + \frac{\beta}{6} \right)^{1/2} + \frac{4\beta}{3\pi} \right]^{1/2}. \quad (11)$$

Determination of β from g' requires knowledge of ε.

Branching frequencies per 10,000 carbon λ_i are determined as

$$\lambda_i = \frac{\beta_i \times 140,000}{M_i}. \quad (12)$$

Figures 4 and 5 show [η] and $\langle R_g^2 \rangle^{1/2}$ versus molecular weight for linear and crosslinked PP. For the linear samples, we obtain the following relations

$$\langle R_g^2 \rangle^{1/2} = 0.0182 \times M^{0.560} \quad (13)$$

and

$$[\eta] = 2.78 \times 10^{-4}\, M^{0.673} \quad (14)$$

The crosslinked samples show reduced $\langle R_g^2 \rangle^{1/2}$ and [η] in the high molecular weight region compared with the linear precursor PP0. For PP518, PP806, and PP1029, this decrease is small but clear. From the data in Figure 5, we find the branching numbers and frequencies. Average branching properties are listed in Table I. As expected the branch numbers (Fig. 6) increase with M in the high molecular fraction and reach a maximum of five branch points per molecule in PP2038. However, since the highly branched fraction is very small the average branching number β_w for PP2038 is only 0.24 branch points/molecule. Branching frequency λ versus M are plotted in Figure 7. The branching frequency λ (branch points/10^4 carbon) generally increases with molecular weight but for PP2038 it passes through a maximum and af-

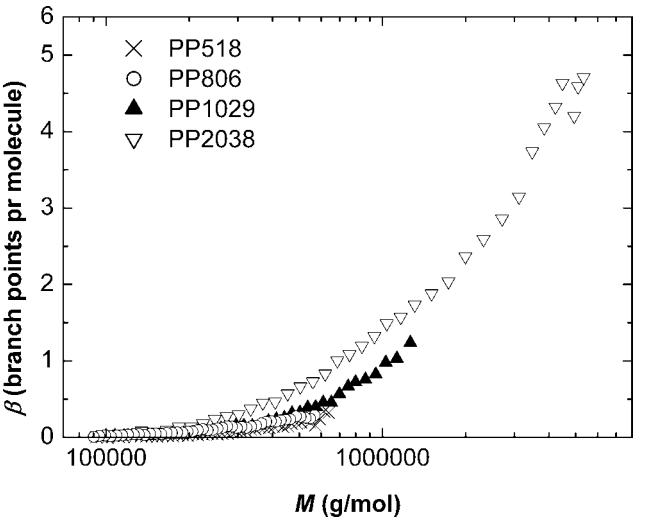

Figure 6 Branching number β versus molecular weight for linear PP crosslinked with different amounts of 1,3-BDSA. The values are computed from the data in Figure 5 and eqs. (8) and (11). The numbers in the legends represent the concentration of crosslinker (ppm).

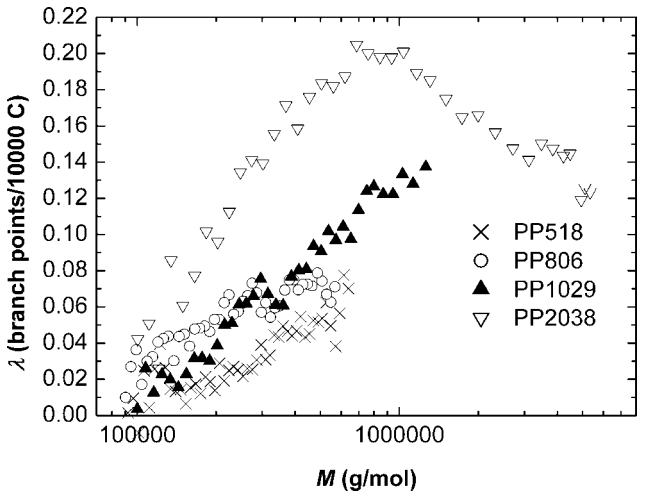

Figure 7 Branching frequency λ versus molecular weight for linear PP crosslinked with different amounts of 1,3-BDSA. The values are calculated from the data in Figure 6 and eq. (12). The numbers in the legends represent the concentration of crosslinker (ppm).

ter that decreases steadily. When we in addition know that the branching number increases strongly in the same molecular weight region the branch length must increase strongly. An equivalent form of the branching frequency distribution was reported for PP crosslinked with peroxydicarbonate in reactive extrusion[4] and we also observed this phenomena in PE crosslinked with 1,3-BDSA. We find this surprising. If the crosslinking process is random and intrachain crosslinking negligible, the branching frequency would increase towards a limiting value characteristic of a fraction with no linear precursors. However, it can be argued that the observed molecular weight dependence of the branching frequency could be predicted by considering the distribution of chain segments in the polymer melt, as in the discussion of random crosslinking above. In a melt under no deformation the polymer chains exist in a random coil conformation. Different chains overlap and form entanglements. Under deformation as during extrusion the chains will be stretched due to entanglements followed by relaxation. However, short chains will relax faster than long chains and be less stretched. Because of this the probability of a chain segment to be positioned next to a segment of another chain will increase with increasing chain length. As a consequence, the ratio of inter- and intrachain crosslinking should increase with the chain length. Intrachain crosslinking can lead to loop structures that resemble LCB and prevent the molecules to expand in the solvent in SEC-analysis resulting in a small $\langle R_g^2 \rangle^{1/2}$. This will give intrachain crosslinked chains an apparently high branching frequency. Such ''fake'' LCB molecules with high λ will be most likely found in the intermediate molecular weight range. On the other hand, ''true'' LCB molecules with large branch point separation (low λ) will most likely be found in the high molecular weight region.

Another and simpler explanation for this decrease in λ at high M is that the formulae used in our branching analyses do not correctly describe the branching structure we study. However, they are the best choices we have.

The crosslinking density ρ defined in eq. (6) and λ (branch point/10,000 C) represent the same phenomena and theoretically they only differ by a scaling factor. Thus, the crosslinking efficiency ν introduced in eq. (7) should also be accessible from λ_w through the relation

$$\lambda_w = \nu \times \{\text{number of crosslinkers pr 10000 carbon}\} \quad (15)$$

In Figure 8, we estimate the crosslinking efficiency of the process by plotting the weight average branching frequencies λ_w versus the content of 1,3-BDSA. As one expects, λ_w increases linearly with the content of 1,3-BDSA. This linearity is useful for the tailoring of materials with a specific branching density. However, from the best fit we find an efficiency of only 6.3%. This is considerably lower than the efficiency of 26% that we predicted from random crosslinking theory. The linearity between λ_w and 1,3-BDSA concentration (Fig. 8) and the relatively poor fit of M_w to random crosslinking theory (Fig. 3) favors the value of 6.3%. In our earlier study, on crosslinking of PE with 1,3-BDSA,[11] we found a

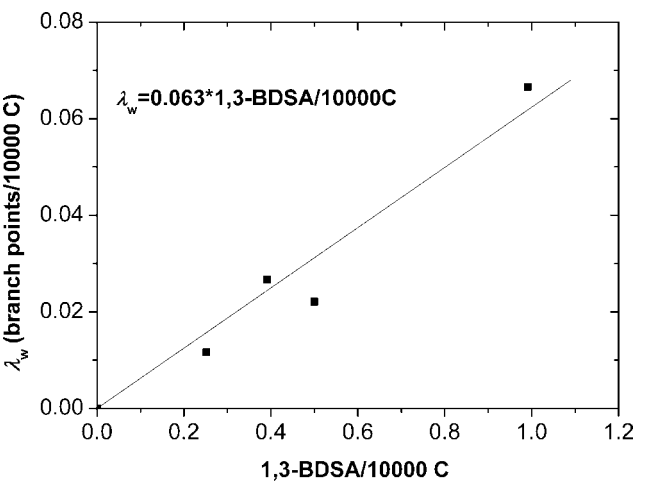

Figure 8 Weight average branching frequency λ_w versus number of 1,3-BDSA molecules/10,000 carbons used in the crosslinking. The data correlates linearly with a slope of 0.063 corresponding to a crosslinking efficiency of 6.3% as defined in eq. (15).

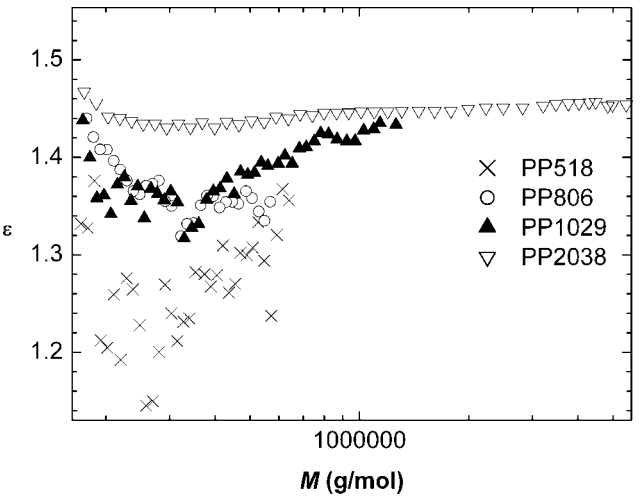

Figure 9 The exponent ε from the relation $g' = g^{\varepsilon}$ versus molecular weight for linear PP crosslinked with 1,3-BDSA.

crosslinking efficiency of 40–60%. This is a dramatic difference that calls for an explanation. We propose two possible explanations. One explanation is that hydrogen bonded to tertiary carbons are more likely to react with triplet nitrenes [Scheme 3(a)] and form macroradicals than hydrogen bonded to secondary carbons. Every second carbon in PP is a tertiary carbon, while linear PE does not contain tertiary carbons. The explanation then implies that a considerable part of the 1,3-BDSA is consumed due to Scheme 3(a). Since no observable chain scission occurs, it also implies that the radical products formed are captured and neutralized by stabilizers. The PP samples contained 800 ppm of the radical stabilizer Irganox 1010® (Hydrocinnamic acid). Stoichiometric calculations reveal that this amount of Irganox 1010® is theoretically capable of neutralizing radicals formed by 782 ppm 1,3-benzenedisulfonyl nitrenes. This could account for most of the difference in efficiency observed in PP and PE. Another explanation is poorer mixing in the case of PP. There are some notable differences in our results on PE and PP supporting this. In the case of PE, the maximum value of β was only 0.6 branch points per molecule but the branched molecules were distributed throughout a large portion of the MWD. In contrast to this, in the case of PP, we find a β maximum of five branch points per molecule, but the branched molecules are mostly found in a high molecular weight tail of the MWD. This suggests that we have obtained poorer mixing of 1,3-BDSA into the PP than we did with PE. The difference in mixing is most likely due to the difference in the process condition. The PE was processed in a medium scale extruder with increasing temperature zones along the screw ensuring mixing before 1,3-BDSA decomposition. In contrast to this the PP discussed here was processed in a mini scale extruder holding the high temperature (200°C) already at the feed section. We believe this could have caused the sulfonyl azide to decompose and form crosslinks before a complete blending was obtained. Incomplete blending would indeed reduce the apparent crosslinking efficiency because crosslink would be formed at neighboring carbons. Also the sulfonyl azide molecules can react with each other instead of forming crosslinks.[10]

The exponents ε relating g' to g are plotted in Figure 9 as a function of M. Averages values are listed in Table I. ε increases with the branching density and tends to approach an upper limit of 1.45. The exponent ε is known to be related to the type of LCB.[37,38] However, we have no self consistent model to explain this relation. Therefore, we only present the values as a reference for comparison of materials formed in similar processes.

Rheological properties

Results from shear creep measurements and dynamic shear measurements at 170, 190, and 210°C are shown in Figures 10–13 and listed in Table II. Dynamic data were adjusted with a temperature dependent shift factor b_T according to the Rouse theory,[39] F10-13

$$b_T = \frac{T_0 \rho_0}{T \rho}, \tag{16}$$

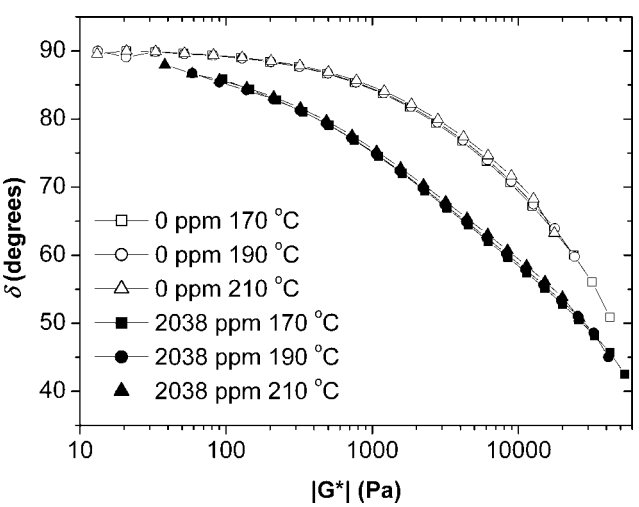

Figure 10 δ versus $|G^*|$ plot of unmodified linear PP and the same material crosslinked with 2038 ppm 1,3-BDSA (highest concentration). Superposition of data from different temperatures indicates that the time temperature superposition principle is valid. For clarity samples of lower crosslinking are omitted, but data from different temperatures superimpose also for PP518, PP806, and PP1029.

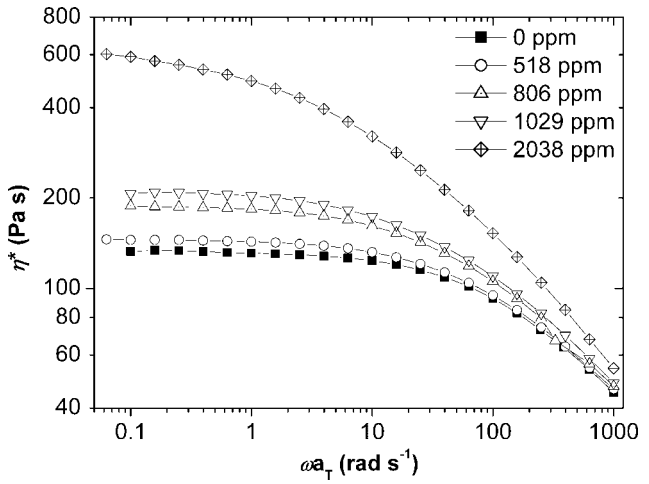

Figure 11 Dynamic shear viscosity versus ωa_T. The plot consists of data from 170, 190, and 210°C shifted to reference temperature 190°C.

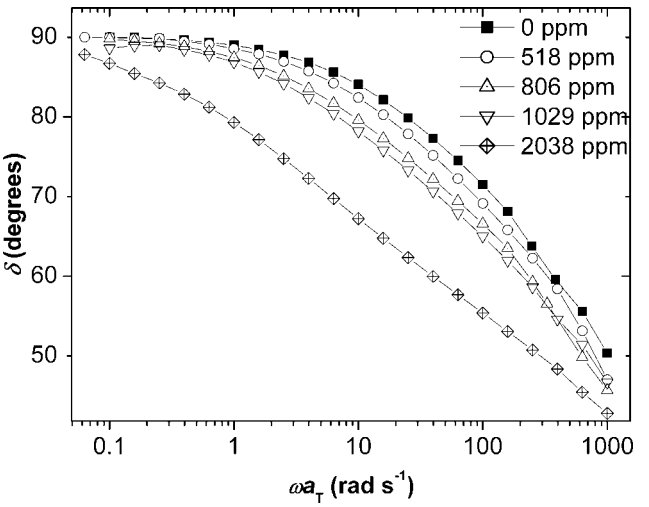

Figure 13 Phase angle δ versus ωa_T. The plot consists of data from 170, 190, and 210°C shifted to reference temperature 190°C.

with density[40]

$$\rho(T) = 0.859\ \exp\left(-6.60 \times 10^{-4}(T - 273.15)\right) \quad (17)$$

Time temperature superposition

For thermorheological simple materials that obey the time temperature superposition principle, data from different temperatures superimpose by shifting frequency or time by a factor a_T given by the Arhenius equation:

$$a_T = \exp\left[\frac{E_a}{R}\left(\frac{1}{T} - \frac{1}{T_0}\right)\right]. \quad (18)$$

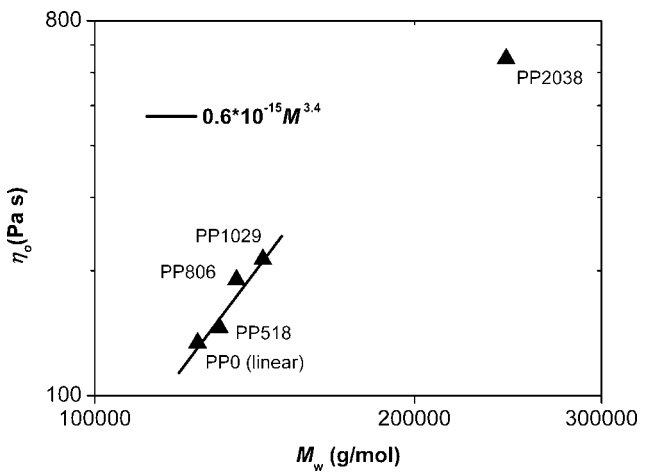

Figure 12 Zero shear viscosity at 190°C versus molecular weight for the linear precursor and crosslinked samples. The full line represents a least squares fit to η_o of PP0, PP518, PP806, and PP1029.

However, the determination of a unique flow activation energy for LCB polymers can be complicated since they often show thermorheological complexity.[30–32] Thermorheological complex materials have modulus dependent activation energy and therefore do not obey the time temperature superposition principle. Thermorheological complexity is revealed by plotting loss angle δ versus storage modulus $|G^*|$,[41] tanδ versus $|G^*|$[32] or G^* versus zero shear viscosity multiplied with frequency $\eta_o\omega$[30] All of these plots are temperature independent if the time temperature superposition principle is valid, and data from different temperatures will superimpose.

Figure 10 shows data for PP0 and PP2038 in a plot of δ versus modulus $|G^*|$ at 170°C, 190°C, and 210°C. Within the accuracy of the data there are no signs of thermorheological complexity. For clarity, the other materials were omitted from Figure 10. They showed no signs of thermorheological complexity. On the basis of this, all data were shifted to the reference temperature 190°C.

Viscosity

Dynamic viscosities η* versus ω are plotted in Figure 11. Zero shear viscosities η_o were determined from creep measurements and from the fitting of dynamic data to the Cross equation[42]

$$\eta^*(\omega) = \frac{\eta_0}{1 + (\lambda\omega)^n}, \quad (19)$$

where η* is the complex viscosity, λ a characteristic time, n an exponent, and ω the frequency. At high temperatures and for samples with few LCB, the viscosities were very low. In that case creep measure-

TABLE II
Rheological Properties (190°C)

Sample	[1,3-BDSA] (ppm)	M_w (10^3g/mol)	η_o (Pa s)	J_e^0 ($Pa^{-1} \times 10^{-4}$)	E_a (kJ/mol)
PP0	0	125	134	2	43
PP518	518	131	146	2	45
PP806	806	136	190	3	44
PP1029	1029	144	213	5	45
PP2038	2038	244	648	23	50

ments gave very uncertain results and the Cross equation was used. In other cases the two methods gave similar results.

The crosslinking clearly enhances the viscosity accompanied by shear thinning. Such shear thinning is desirable in processing. However, the viscosity enhancement is far from as large as often observed for LCB.[5,7,8,24] The viscosity enhancement is more comparable to that observed in a case of PP crosslinked peroxydicarbonates.[21] That the viscosity enhancement is indeed moderate can be revealed by examination of the molecular weight dependence of η_o (Fig. 12). For concentrations up to 1029 ppm 1,3-BDSA, the molecular weight dependence of η_o follows the relation $0.6 \times 10^{-15}\ M_w^{3.4}$. An exponent close to 3.4 is expected for linear materials. The most branched material PP2038 actually has lower viscosity than expected from this relation. This is in contrast to the strong viscosity enhancement that is normally observed for polymers with low levels of LCB.[26] However, this behavior can be explained by comparison with the SEC results. From the SEC analysis we argued that the crosslinking process has resulted in a locally high branching density. In others words, we imagine a rather large number of linear chains blended with a few branched chains of which some contain several branches. If the distance between branch points in such highly branched molecules are low compared to the entanglement molecular weight they would contribute less to the viscosity than linear chains. An example of this is LDPE. Because of its dense branch structure, LDPE can have reduced zero shear viscosity compared to linear PE of same molecular weight.[26] In that context it is also noteworthy that molecular weight between entanglements M_e for isotactic PP is rather high[43] (6900 g/mol). In comparison, M_e of PE[44] is only 1300 g/mol. Thus, for isotactic PP rather long branches are required to form strong entanglements.

The phase angle δ (Fig. 13) and shear recoverable compliance J_e^o (Table II) are two entanglement sensitive parameters that is often strongly influenced by LCB. δ starts to form a plateau at 2038 ppm 1,3-BDSA, which is a clear sign of strong entanglements due to LCB. J_e^o is very low for the linear material but increases strongly at concentrations above 1029 ppm.

Flow activation energy

Increased flow activation energy E_a is a typical sign of LCB E_a.[27,29,30] However, as discussed earlier, thermorheological complexity makes determination of E_a difficult.

Wood-Adams and Costeux[30] have demonstrated that the activation energy spectrum of a thermorheological complex polymer can be calculated from the storage modulus. They also point out that the activation energy found from the zero shear viscosity is a weighted average of the activation energy spectrum, and therefore is suitable for comparison of different materials. To facilitate comparison with other LCB materials, we follow this suggestion and calculate E_a (Table II) from η_o. We found $E_a = 43$ kJ/mol for linear PP. This value is in accordance with values reported for linear isotactic PP. E_a for the branched samples are close to the value for the linear except for PP2038 for which it increases to 50 kJ/mol.

CONCLUSIONS

The molecular structure and rheology of an isotactic PP modified with 1,3-BDSA in reactive extrusion were studied by SEC and shear rheometry. The results show that crosslinking and formation of LCB are the result of the modification and no degradation could be observed. However, the observed crosslinking efficiency was smaller than that observed for PE in our earlier studies. We propose that this could be caused by differences in process conditions or by differences in nitrene reactivity in PP and PE combined with interaction with stabilizers.

Further research is needed to optimize the use of 1,3-BDSA for crosslinking. Optimization of equipment and process conditions for improved blending and crosslinking efficiency is an obvious task to address, as well as evaluating the effect of stabilizers. On the characterization side, studies on extensional flow behavior would probably reveal interesting information.

References

1. Gahleitner, M. Prog Polym Sci 2001, 26, 895.
2. Borve, K. L.; Redford, K.; Skattum, M.; Haavaldsen, J. T. World Pat. 2001066632 (2001).
3. Andreassen, E.; Borve, K. L.; Rommetveit, K.; Redford, K. Soc Plast Eng Annu Tech Conf 1999, 57, 2104.
4. Lagendijk, R. P.; Hogt, A. H.; Buijtenhuijs, A.; Gotsis, A. D. Polymer 2001, 42, 10035.
5. Schulze, D.; Trinkle, S.; Mülhaupt, R.; Friedrich, C. Rheol Acta 2003, 42, 251.
6. Ratzsch, M. J Macromol Sci Pure Appl Chem 1999, 36, 1759.
7. Ye, Z.; AlObaidi, F.; Zhu, S. Ind Eng Chem Res 2004, 43, 2860.
8. Walter, P.; Trinkle, S.; Lilge, D.; Friedrich, C.; Mulhaupt, R. Macromol Mater Eng 2001, 286, 309.
9. Weng, W.; Hu, W.; Dekmezian, A. H.; Ruff, C. J Macromol 2002, 35, 3838.
10. Jorgensen, J. K.; Ommundsen, E.; Stori, A.; Redford, K. Polymer 2005, 46, 12073.
11. Jorgensen, J. K.; Stori, A.; Redford, K.; Ommundsen, E. Polymer 2005, 46, 12256.
12. Breslow, D. S.; Spurlin, H. M. U.S. Pat. 3,203,937 (1965).
13. Breslow, D. S.; Sloan, M. F.; Newburg, N. R.; Renfrow, W. B. J Am Chem Soc 1969, 91, 2273.
14. Breslow, D. S. In Nitrenes, 1st ed.; Lwowski, W., Ed.; Wiley: New York, 1970, p 245.
15. Yasuda, N.; Yamamoto, S.; Wada, Y.; Shozo, Y. J Polym Sci Part A: Polym Chem 2001, 39, 4196.
16. Bubeck, R. A. Mat Sci Eng R 2002, 39, 1.
17. Hingmann, R.; Marczinke, B. L. J Rheol 1994, 38, 573.
18. Kurzbeck, S.; Oster, F.; Munstedt, H.; Nguyen, T. Q.; Gensler, R. J Rheol 1999, 43, 359.
19. Lu, B.; Chung, T. C. Macromolecules 1999, 32, 8678.
20. Gotsis, A. D.; Zeevenhoven, B. L. F.; Hogt, A. H. Polym Eng Sci 2004, 44, 973.
21. Gotsis, A. D.; Zeevenhoven, B. L. F.; Tsenoglou, C. J Rheol 2004, 48, 895.
22. Tsenoglou, C. J.; Gotsis, A. D. Macromolecules 2001, 34, 4685.
23. McLeish, T. C. B. Curr Opin Solid State Mater Sci 1997, 2, 678.
24. Wang, W. J.; Ye, Z.; Fan, H.; Li, B. G.; Zhu, S. Polymer 2004, 45, 5497.
25. Beer, F.; Capaccio, G.; Rose, L. J. J Appl Polym Sci 1999, 73, 2807.
26. Gabriel, C.; Munstedt, H. Rheol Acta 2002, 41, 232.
27. Lohse, D. J.; Milner, S.T.; Fetters, L. J.; Xenidou, M.; Hadjichristidis, N.; Mendelson, R. A.; Garcia-Franco, C. A.; Lyon, M. K. Macromolecules 2002, 35, 3066.
28. Gell, C. B.; Graessley, W. W.; Efstratiadis, V.; Pitsikalis, M.; Hadjichristidis, N. J Appl Polym Sci 1997, 35, 1943.
29. Malmberg, A.; Gabriel, C.; Steffl, T.; Munstedt, H.; Loefgren, B. Macromolecules 2002, 35, 1038.
30. Wood-Adams, P.; Costeux, S. Macromolecules 2001, 34, 6281.
31. Graessley, W. W. Macromolecules 1982, 15, 1164.
32. Mavridis, H.; Shroff, R. N. Polym Eng Sci 1992, 32, 1778.
33. Huglin, M. B. Light Scattering From Polymer Solutions, 1st ed.; Academic Press: New York, 1972.
34. Frank, R.; Frank, L.; Ford, N. C. In Characterization of polymers: Hyphenated and Multidimensional Techniques; Prowder, T., Ed.; American Chemical Society: Washington, DC, 1995, p 109.
35. Macosko, C. W.; Miller, D. R. Macromolecules 1976, 9, 199.
36. Tobita, H. Macromol Theory Simul 1996, 5, 1167.
37. Zimm, B. H.; Stockmayer, W. H. J Chem Phys 1949, 17, 1301.
38. Tackx, P.; Tacx, J. C. J. F. Polymer 1998, 39, 3109.
39. Ferry, J. D. Viscoelastic Properties of Polymers, 3rd ed.; Wiley: New York, 1980.
40. Mark, J. E. Physical Properties of Polymers Handbook; American Institute of Physics: New York, 1996.
41. Trinkle, S.; Walter, P.; Friedrich, C. Rheol Acta 2002, 41, 103.
42. Cross, M. M. J Appl Polym Sci 1969, 13, 765.
43. Eckstein, A.; Suhm, J.; Friedrich, C.; Maier, R.-D.; Sassmannshausen, J. Macromolecules 1998, 31, 1335.
44. Raju, V. R.; Rachapudy, H.; Graessley, William, W. J Polym Sci Phys Ed 1979, 17, 1223.